sciendo

DOI: 10.2478/ata-2025-0018

Acta Technologica Agriculturae 3
Nitra, Slovaca Universitas Agriculturae Nitriae, 2025, pp. 141–148

DESIGN, FABRICATION, AND PERFORMANCE EVALUATION OF SOLAR DRYING CHAMBER USED FOR APPLE SLICES

Halefom KIDANE[1], Istvan FARKAS*[2], Janos BUZÁS[2]

[1]Hungarian University of Agriculture and Life Sciences, Doctoral School of Mechanical Engineering, Gödöllő, Hungary, Abrha.Halefom.Kidane@phd.uni-mate.hu
[2]Hungarian University of Agriculture and Life Sciences, Institute of Technology, Department of Mechatronics, Gödöllő, Hungary, Buzas.Janos@uni-mate.hu
*correspondence: Farkas.Istvan@uni-mate.hu

The manuscript discusses the design, fabrication, and performance evaluation of a solar drying chamber specifically for drying golden apple slices, highlighting the importance of solar energy in agricultural product preservation. The objectives of the study were to design, fabricate, and evaluate the thermal performance and drying efficiency of solar drying systems and to identify the best thin-layer model for describing the drying kinetics of golden apple slices. The study revealed significant temperature variations in the trays during the drying process, with bottom trays experiencing higher moisture loss compared to other trays. The drying process of golden apples slices occurs entirely in the falling rate, and the Midilli and Kucuk model was found the best model to describe the drying kinetics, accurately capturing the drying behaviour and predicting of golden apple slice.

Keywords: drying kinetics; moisture ratio; falling period; thermal performance; thin layer model

The world faces three major challenges: ensuring reliable energy, achieving food security, and combating global warming. The food industry accounts for 30% of global greenhouse gas emissions, while food waste intensifies global warming, with 1.3 billion tons discarded annually. A potential solution to reducing emissions from both the food industry and food waste is the adoption of effective food preservation methods, such as drying, combined with the use of renewable energy sources (Hassan et al., 2023). Drying is one of the most effective methods to reduce additional costs, as it decreases the weight of the product to less than one-third of its initial weight. Furthermore, lowering moisture content helps minimise microbial and enzymatic activities during storage, thereby significantly extending the product's shelf life (Bouhdjar et al., 2020; Meisami-asl and Rafiee, 2009). The primary objectives of drying include preventing decay and spoilage, extending shelf life, reducing storage, handling, and transportation costs, and enhancing product quality (Odewole and Falua, 2021). The increasing cost and limited availability of fossil fuels are driving a shift towards solar energy for drying processes, as it offers a free and readily accessible alternative to reduce fuel consumption (Lingayat et al., 2017; Atalay and Cankurtaran, 2021). Solar dryers can significantly contribute to reducing post-harvest losses in both developed and developing nations, while also enhancing value addition (Musembi et al., 2016; Hasan and Langrish, 2016).

The research introduces advancements in the solar drying technology for agricultural products, particularly through the innovative design, fabrication, and testing of a solar dryer. The research evaluates the key performance metrics such as moisture loss and drying kinetics, various thin-layer drying models for describing apple slice drying, and analyses colour changes to understand the impact of drying conditions on product quality. The study provides valuable insights into the thermal behaviour of solar drying systems, offering a basis for future optimisation in agricultural drying practices.

Material and methods

Study area

The solar air heater and the drying chamber, as depicted in Figs 1–2, were designed and fabricated at the Hungarian University of Agriculture and Life Sciences (47° 35' 39" N and 19° 21' 59" E). Golden apple slices were used as drying sample. The experiment was conducted on selected sunny days of July to August 2024.

However, in this case, three sunny days were utilised to analyse the thermal performance of the drying system and to model the drying behaviour of the golden apple slices.

Tools used during the experiment

A solar air heater with a diffuser-shaped inlet (1.25 × 0.5 m) was designed, incorporating a 4 mm thick plexiglass sheet, and a 1.2 mm thick copper absorber plate was integrated with the drying chamber. The drying chambers were made up from polystyrene (XPS) boards. The doors, which are used to close the dryers, were fabricated from Akrylon XT acrylic sheets. The dryers are equipped with four trays inside. The trays are made up from fiberglass. The dimension of tray is 0.48 × 0.50 m, arranged with a uniform spacing of 0.1 m. The chamber's inlet and outlet have a circular cross-section with a diameter of 0.1 m and an axial length of 0.2 m. Four trays were filled with apple slices, each with a thickness ranging from 4 mm to 6.5 mm and a diameter between 5 cm

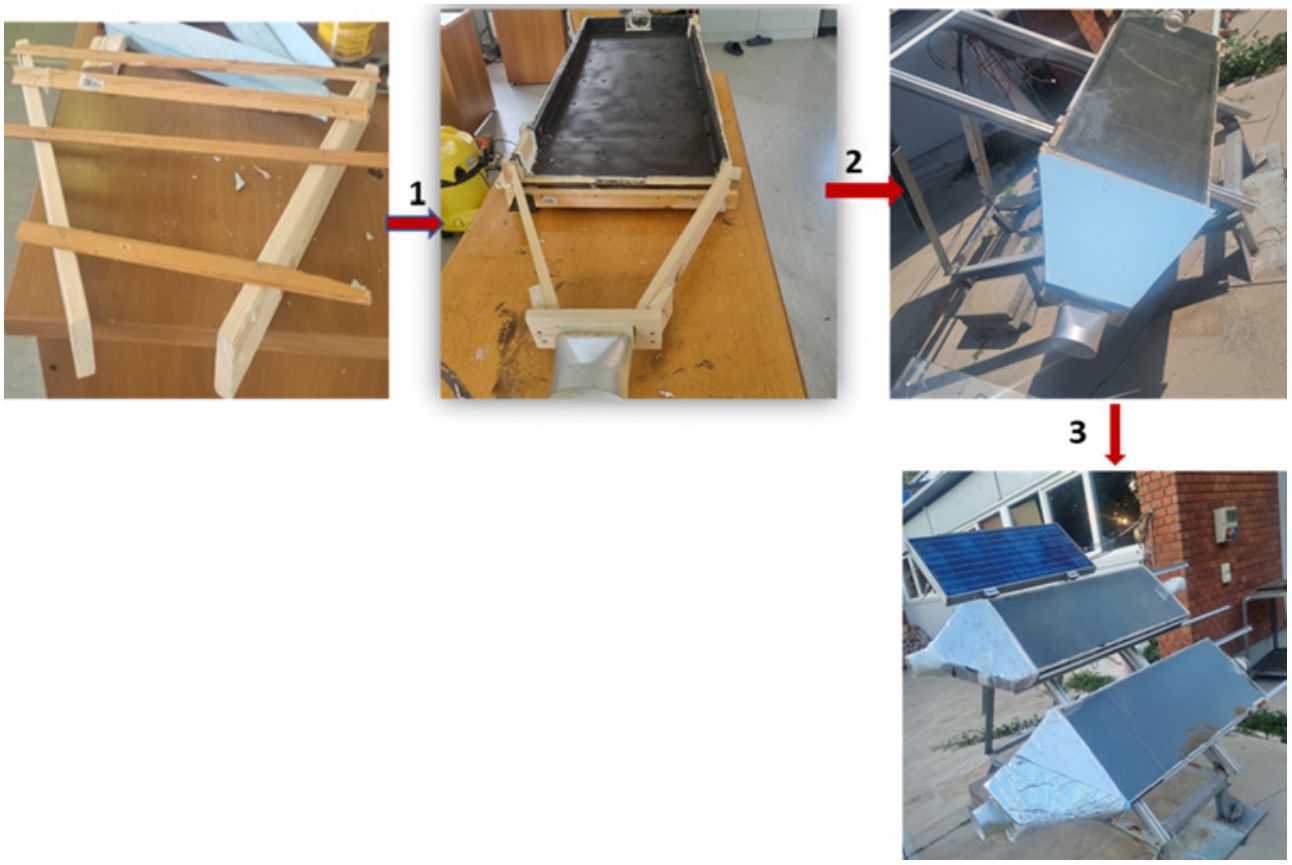

Fig. 1 Manufacturing process of the solar air heaters

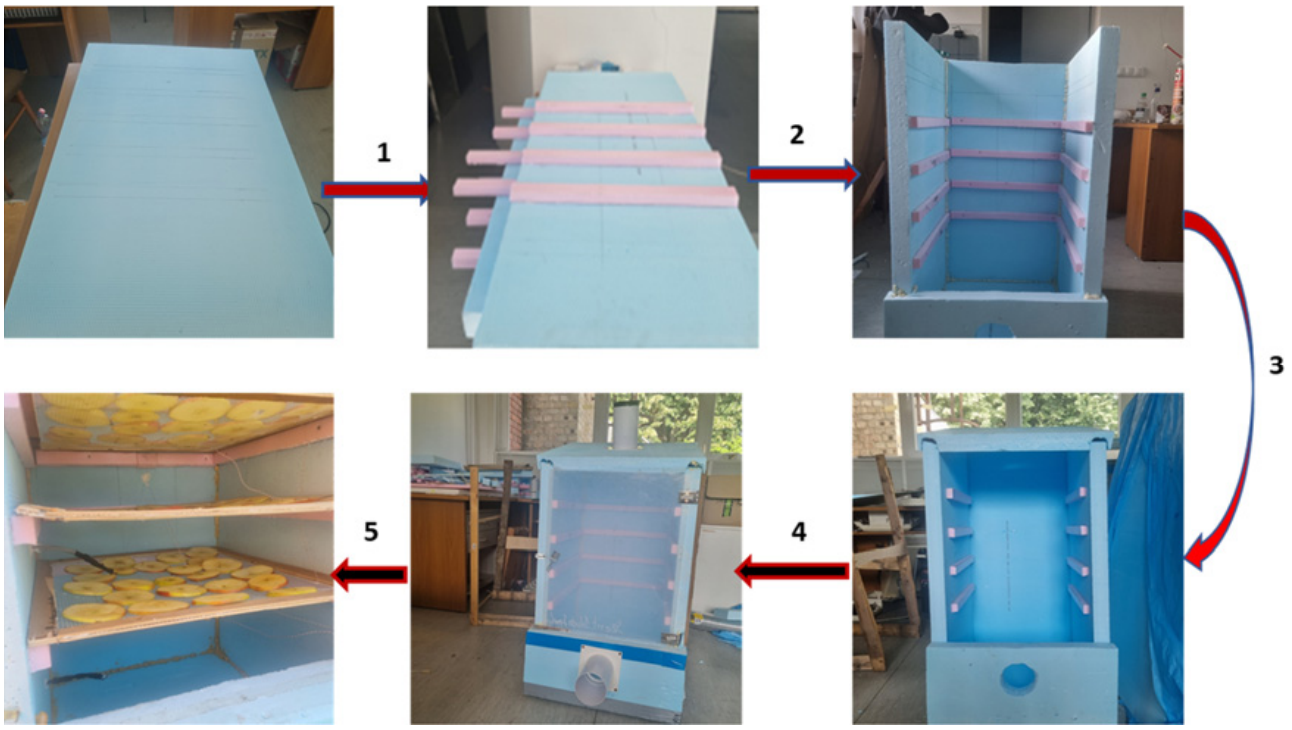

Fig. 2 Manufacturing process of the drying chambers

and 8.35 cm. The slices were carefully laid out to ensure even distribution across the trays.

Data collection

A humidity sensor (model: HIH-40000-004, produced by Honeywell, USA) with an accuracy of ±3.5% and an operational range of 0% to 100% RH was used to measure humidity. The pressure and flow rate sensor (model: SDP816-500Pa, manufactured by Sensirion, Switzerland) with an accuracy of ±5 millibar and a range of -500 to 500 Pa was provided with two units. Temperature was monitored using a resistance temperature detector (RTD) sensor (PT-100) with an accuracy of ±0.1 °C at 0 °C, operating within a range of -75 °C to 250 °C. Solar radiation was measured using a pyranometer (model: Kipp and Zonen CM11, produced by Kipp and Zonen, The Netherlands) with an accuracy of ±0.1 Wm^{-2} and a range of 1 to 4000 Wm^{-2}.

Performance evaluation of solar drying system components

The detailed calculations used for sizing the drying components are not included here; only the basic performance indicators and parameters are provided. Additionally, the fundamental characterisation methods of the sample being dried are discussed.

Energy analysis of solar air heater

The basic performance indicators are discussed in the following sections.

The efficiency of the solar air heater (η_{SAH}) is computed by employing the following equation (Mugi and Chandramohan, 2021):

$$\eta_{SAH} = \frac{\dot{m}_a \, C_{pa} \, (T_{SAHo} - T_{amb})}{A_{SAH} \, \tau\alpha I_r} \quad (1)$$

where: $\dot{m}_a$ – the mass flow rate of heated air ($kg \cdot s^{-1}$); C_p – specific heat capacity ($kJ \cdot kg^{-1} \cdot K^{-1}$); α –absorbance of the glass cover = 0.85; τ – transmittance of the glass cover = 0.95; A_{SAH} – the surface area of the solar air heater; T_{SAHo} – temperature leaving the SAH

The heat obtained (*Qu*) from the solar air heater and given by Mugi and Chandramohan (2021):

$$Qu = \dot{m}_a \, C_{pa} \, (T_{SAHo} - T_{amb}) \quad (2)$$

where: T_{amb} – ambient temperature (°C)

The specific heat ($J \cdot kg^{-1} \cdot °C^{-1}$) of air was calculated using the Eq. (3) provided by (Ekka and Palanisamy, 2020):

$$C_{pa} = 999.2 + 0.1434 \, T_{av} + 1.101 \cdot 10^{-4} \, T_{av}^2 - 6.758 \, 10^{-8} \, T_{av}^3 \quad (3)$$

The system efficiency of a solar dryer quantifies the effectiveness of utilising input energy (solar radiation) for product drying. For forced flow, we are considering the power of the available auxiliary devices like a fan, pump, or any other external energy supplier (Rabha et al., 2017).

The efficiency of the forced type of solar dryer (η_{of}) is given as follows:

$$\eta_{of} = \frac{m_{rv} \, h_{fg}}{I_r A_d + Fp} \quad (4)$$

where: h_{fg} – the latent heat of vaporisation ($kJ \cdot kg^{-1}$); m_{rw} – the mass of water removed; I_r – solar intensity striking on the surface of SAH ($W \cdot m^{-2}$); *Fp* – the power of the fan (W); A_d – the area of the drying chamber (m^2)

The quantity m_{rw} is given by the following equation:

$$m_{rw} = m_i - m_f \quad (5)$$

where: m_f – the final mass of the dried product (g); m_i – the initial mass of the product (g)

The value of the latent heat of vaporisation (h_{fg}) of water can be estimated using the following formula (Forson et al., 2007):

$$h_{fg} = \left(R_g T_c T_b \times \ln\left(\frac{P_{cr}}{10^5} \right) \right) \times \frac{(T_{cr} - T_p)^{0.38}}{(T_{cr} - T_b)^{1.38}} \quad (6)$$

where: P_{cr} – the critical pressure of water (2.206×10^7 Pa); R_g – gas constant for water vapour ($461.5 \, J \cdot kg^{-1} \cdot K^{-1}$); T_b – temperature at which water boils under standard atmospheric pressure (°C); T_{cr} – the critical temperature of water (377 °C); T_p – the temperature of product (°C)

Mathematical model of products

Numerous parameters are employed to characterise the drying behaviour and conditions of products processed in solar drying chambers, including temperature, humidity, air velocity, moisture content, and moisture ratio. These parameters are critical for optimising the drying process, ensuring energy efficiency and preserving the quality of dried products.

Moisture content

To assess the moisture content (*Mc*) of the samples on a wet basis throughout the day as they undergo the drying process (Rajesh et al., 2024):

$$Mc = \frac{m_w - m_s}{m_i} \quad (7)$$

where: m_w – the mass of the wet sample at time *t* (kg); m_s – the mass of the dried sample at time *t* (kg); m_i – the initial mass of the sample (kg)

Moisture ratio

The moisture ratio (*MR*) of the product is calculated using Eq. (8) (Doymaz and Ismail, 2011):

$$MR = \frac{M_t - M_e}{M_0 - M_e} \quad (8)$$

where: M_t, M_0, and M_e – the moisture content at any given time during drying (kg of water per kg of dry matter), the initial moisture content (kg of water per kg of dry matter), and the equilibrium moisture content (kg of water per kg of dry matter), respectively

The products were not continuously subjected to consistent relative humidity and temperature, and the values of M_e were significantly smaller than M_t or M_0. As a result, the error caused by simplification is insignificant. Thus, Eq. (8) will be simplified to Eq. (9) (Doymaz, 2007; El-Beltagy et al., 2007):

$$MR = \frac{M_t}{M_0} \quad (9)$$

Thin-layer drying models

To choose an appropriate thin-layer model for drying apple slices in all days, four thin-layer mathematical models (listed in Table 1) were utilised to compare the experimental *MR* and theoretical moisture ratio data over time. The R^2 value approaching 1 signifies a strong relationship between the model and the data, whereas an R^2 value close to 0 indicates a weak fit. A model with lower *RMSE* and x^2 values is considered to have better performance compared to one with higher *RMSE* and x^2 (Ullah et al., 2022).

Results and discussion

Solar radiation, ambient temperature variation, and humidity analysis

The average solar radiation levels recorded over the three days were 854.34 W·m^{-2}, 868.91 W·m^{-2}, and 897.93 W·m^{-2} for days 1, 2, and 3, respectively. During the same period, the average temperatures were 30.73 °C, 26.38 °C, and 31.4 °C for days 1, 2, and 3, respectively. The average humidity levels varied across the drying chamber, with day 1 recording 41.08%, 46.73%, and 48.99% at the inlet, middle, and outlet, respectively. On day 2, the humidity levels were 46.67%, 60.70%, and 63.32% at the inlet, middle, and outlet, while day 3 showed 38.99%, 47.55%, and 48.51% at the same locations.

Performance analysis of the system

The efficiency of the solar air heater was analysed over three days, as shown in Fig. 3(a). Day 3 recorded the highest overall peak, followed by day 1 and day 2. Mid-day performance fluctuated, with day 1 and day 2 experiencing drops due to external factors. Late-day performance exhibited earlier peaks but maintained high efficiency until 16:00. Day 3 outperformed the others, achieving the highest maximum efficiency and demonstrating a gradual improvement in performance, indicating optimal conditions and system functionality. The average efficiency was 45.36%, 44.82%, and 57.07% for day 1, day 2, and day 3, respectively.

The efficiency of the drying chamber over three days was analysed, as shown in Fig. 3(b). The dryer's efficiency varied significantly across the three days, with day 3 being the most efficient due to higher and more consistent solar radiation.

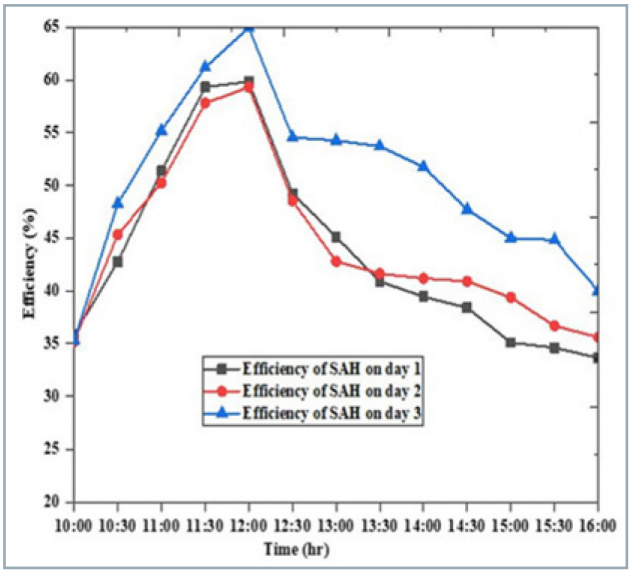

Fig. 3a Average efficiency of the solar air heater over the three days

Table 1 Selected thin-layer models and statical metrices

Name of the model	Model equation	Statistical tools and corresponding formula
Newton	$MR = \exp(-kt)$	$R^2 = \frac{n\sum_{i=1}^{n} x_i y_i - \left(\sum_{i=1}^{n} x_i\right)\left(\sum_{i=1}^{n} y_i\right)}{\sqrt{\left[n\sum_{i=1}^{n} x_i^2 - \left(\sum_{i=1}^{n} x_i\right)^2\right]}\sqrt{\left[n\sum_{i=1}^{n} y_i^2 - \left(\sum_{i=1}^{n} y_i\right)^2\right]}}$
Page model	$MR = \exp(-t^n)$	$x^2 = \frac{\sum_{i=1}^{n}(x_i - y_i)^2}{n-c}$
Modified page	$MR = \exp(-(kt)^n)$	$RMSE = \sqrt{\sum_{i=0}^{n}\frac{(x_i - y_i)^2}{n}}$
Midilli and Kucuk	$MR = a\exp(-kt^n) + bt$	

Source: Doymaz, 2013; Mellalou et al., 2023

k, *a*, *b*, and *n* – empirical constants derived from experiments; *t* – time; *c* – the number of constantans in model; R^2 – coefficient of determination (%); *RMSE* – root mean square error (%); *x* – experimental data; x^2 – chi-square; *y* – predicted (calculated) data

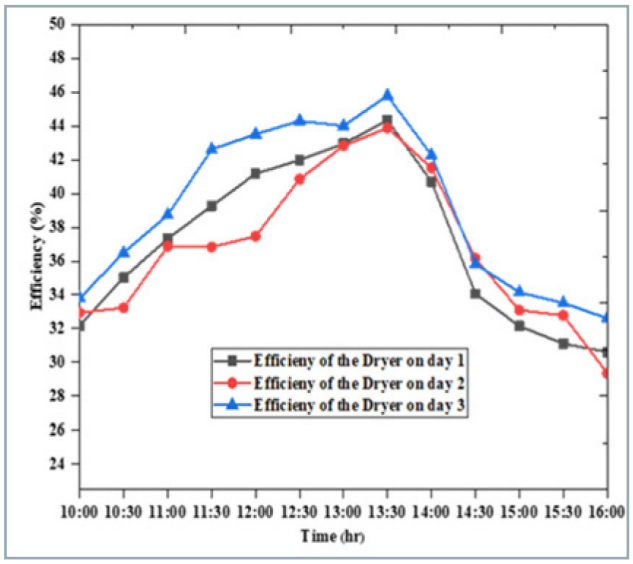

Fig. 3b Average efficiency of the solar drying chamber over the three days

Day 1 also performed well, while day 2 was less efficient, likely due to the environmental factors such as humidity or cloud cover. These results highlight the importance of solar radiation and ambient conditions in determining the efficiency of solar drying systems. Future improvements could focus on optimising the system to maintain consistent performance even under less ideal conditions.

Moisture analysis

Mass reduction during the drying period over the three day is shown in Fig. 4a, b, c. Day 3 exhibits a mass reduction pattern similar to day 1 and day 2, characterised by a rapid initial loss followed by a gradual decline. However, the overall mass reduction on day 3 appears slightly greater, likely due to improved drying conditions. This can be attributed to more favourable environmental conditions on day 3, characterised by higher solar radiation intensity and ambient temperatures, along with lower humidity compared to other days.

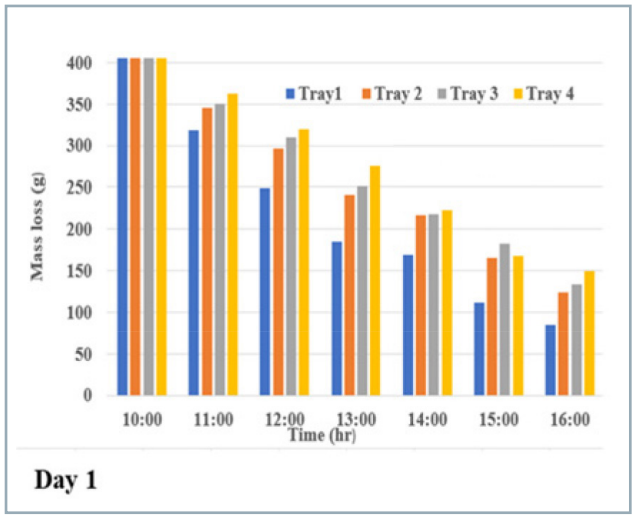

Fig. 4a Weight loss with time across the trays

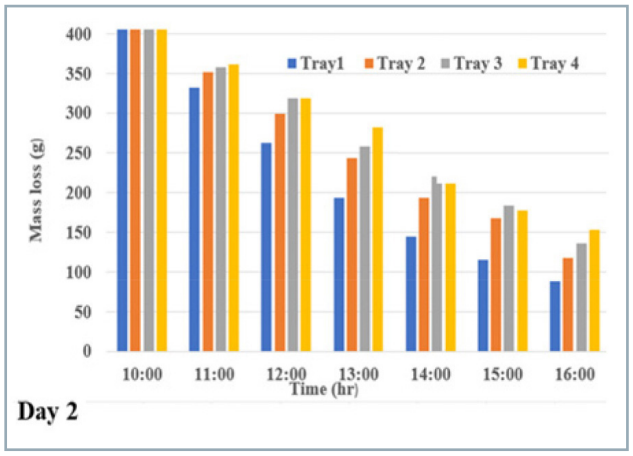

Fig. 4b Weight loss with time across the trays

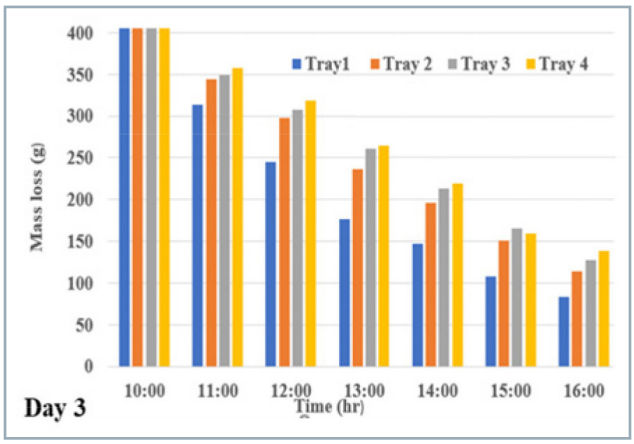

Fig. 4c Weight loss with time across the trays

Moisture ratio and drying curves

To calculate the moisture ratio (*MR*) and drying curves, the total mass of the drying chamber was considered instead of individual tray measurements for simplicity. Hourly mass readings were recorded, starting with an initial mass of 1620 g (405 g) at 10:00 AM, and subsequent measurements followed. As presented in Fig. 5(a), the moisture ratio (*MR*) values for three days of drying have been investigated at hourly intervals starting from 10:00 AM. The initial *MR* at 10:00 AM for all days is 1, which represents the fully saturated condition of the material (maximum moisture content relative to dry weight). As drying progresses, *MR* decreases steadily over time, indicating moisture loss. The drying curve data demonstrate a typical drying process characterised by an initial rapid phase and an intermediate slowing phase, as shown in Fig. 5(b).

The drying kinetics of materials involves two primary phases: the constant rate period and the falling rate period. During the constant rate period, moisture content decreases steadily as surface moisture evaporates, driven by the external factors such as temperature and air velocity. This phase is followed by the falling rate period, which consists of two stages: the initial falling rate period, where the rate of moisture removal slows compared to the constant rate, and the curvilinear falling rate period, marked by a further

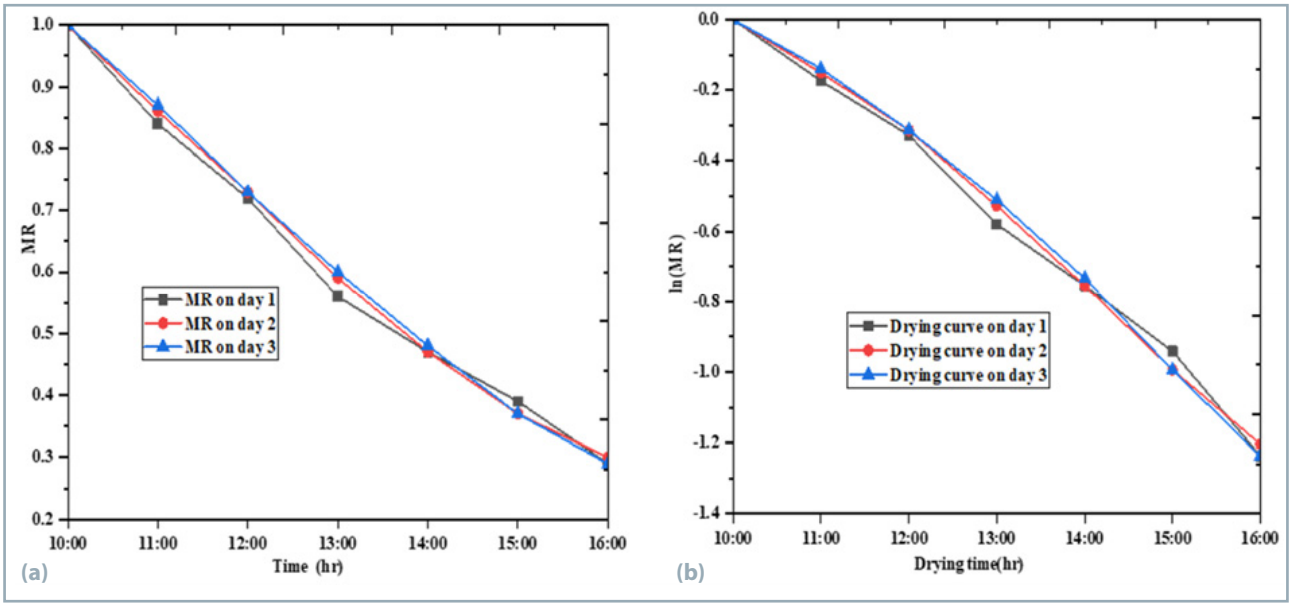

Fig. 5 Moisture ratio (a) and drying curve (b) of the apple slices

gradual and curvilinear reduction in moisture content (Erbay and Icier, 2010).

Thus, in our case shown in Fig. (5b), the drying process entirely occurs in the falling period.

Selecting the best fitting model

As shown in Table 2, the Midilli and Kucuk mathematical models consistently demonstrate strong performance across all days, with higher R^2 values and lower x^2 and *RMSE* compared to the Newton, Page, and Modified Page models.

The Midilli and Kucuk equation, selected to describe the drying behaviour of the golden apple, is presented in Eq. (10):

$$MR = 2.82 \exp(-5.02\, t^{1.80}) + 0.0029\, t \quad (10)$$

The predicted values of the moisture ratio (*MR*) using the model and the experimental values are shown in Fig. 6. As illustrated in Fig. 6, the predicted and actual values are well-fitted, demonstrating the model's accuracy and reliability in capturing the experimental data trends.

Table 2 Statistical results of drying curve models for apple slice moisture data of three days

Model Name	Constants	R^2	*RMSE*	x^2
Day 1				
Newton	$k = 1.1$	0.999249	0.07682	0.5306
Page model	$n = 0$	–	1.3977	7.8150
Modified Page	$k = 1, n = 1$	0.9991	0.2611	0.13637
Midilli and Kucuk	$a = 2.82, b = 0.0029, k = 5.02$, n = 1.80	**0.9969**	**0.03105**	**0.00385**
Day 2				
Newton	$k = 1.1$	0.9974	0.4980	0.2480
Page model	$n = 0$	–	5.6015	31.3778
Modified Page	$k = 1, n = 1$	0.9972	0.2451	0.05842
Midilli and Kucuk	$a = 2.82, b = 0.0029, k = 5.02, n = 1.80$	**0.9985**	**0.0289**	**0.0033**
Day 3				
Newton	$k = 1.1$	0.9944	0.5002	0.2502
Page model	$n = 0$	–	5.5915	31.2649
Modified Page	$k = 1, n = 1$	0.994	0.2457	0.1208
Midilli and Kucuk	$a = 2.82, b = 0.0029, k = 5.02, n = 1.80$	**0.9989**	**0.0308**	**0.0038**

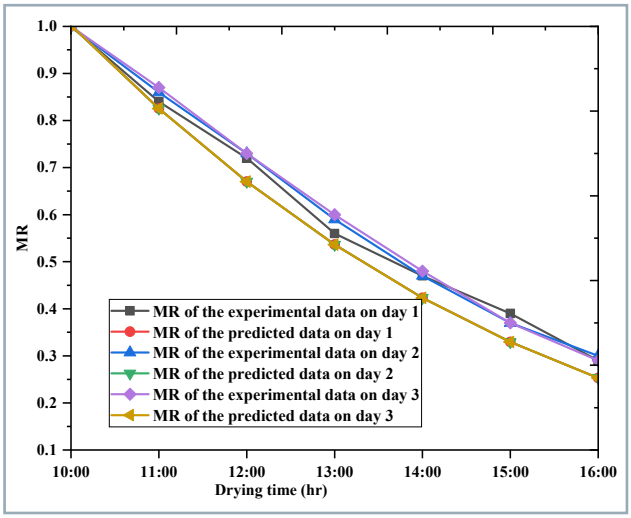

Fig. 6 Moisture ratio (*MR*) of the experimental results vs predicted results using the Midilli and Kucuk models

Conclusion

The study assessed the thermal performance of a solar drying system using golden apple slices as the drying sample. Key findings highlight that higher solar radiation and ambient temperatures significantly enhance drying efficiency, while lower humidity levels further improve drying rates. Additionally, tray positioning was found to play a crucial role in moisture loss, with the bottom trays experiencing the highest mass reduction compared to the top trays. Among the tested models, the Midilli and Kucuk model emerged as the most accurate in describing the drying kinetics of apple slices, providing a reliable tool for predicting moisture loss. Overall, the research underscores the potential of solar drying systems as a sustainable and energy-efficient alternative to conventional drying methods, particularly for preserving agricultural products.

Future studies should extend the experimental period to include diverse weather conditions and test a wider range of agricultural products. Optimising the chamber's design, such as improving airflow and insulation, could enhance efficiency. Economic and environmental analyses are needed to assess feasibility for large-scale use.

Acknowledgment

The authors would like to acknowledge financial support provided by the Stipendium Hungaricum Program and by the Doctoral School of Mechanical Engineering, Hungarian University of Agriculture and Life Sciences, Gödöllő, Hungary. This research received a grant from the Foundation of Environmental-friendly and Renewable Energy Resources, Hungary, no. 4/2024/12/19.

References

ATALAY, H. – CANKURTARAN, E. 2021. Energy, exergy, exergo-economic and exergo-environmental analyses of a large scale solar dryer with PCM energy storage medium. In Energy, vol. 216, article no. 119221. DOI: https://doi.org/10.1016/j.energy.2020.119221

BOUHDJAR, A. – SEMAI, H. – BOUKADOUM, A. – ELMOKRETAR, S. – MAZARI, A. – SEMIANI, M. – AMARI, A. 2020. Improved procedure for natural convection garlic drying. In Acta Technologica Agriculturae, vol. 23, no. 2, pp. 92–98. DOI: https://doi.org/10.2478/ata-2020-0015

DOYMAZ, I. 2007. Air-drying characteristics of tomatoes. In Journal of Food Engineering, vol. 78, no. 4, pp. 1291–1297. DOI: https://doi.org/10.1016/j.jfoodeng.2005.12.047

DOYMAZ, I. 2013. Experimental study on drying of pear slices in a convective dryer. In International Journal of Food Science and Technology, vol. 48, no. 9, pp. 1909–1915. DOI: https://doi.org/10.1111/ijfs.12170

DOYMAZ, I. – ISMAIL, O. 2011. Drying characteristics of sweet cherry. In Food and Bioproducts Processing, vol. 89, no. 1, pp. 31–38. DOI: https://doi.org/10.1016/j.fbp.2010.03.006

EKKA, J. P. – PALANISAMY, M. 2020. Determination of heat transfer coefficients and drying kinetics of red chilli dried in a forced convection mixed mode solar dryer. In Thermal Science and Engineering Progress, vol. 19, article no. 100607. DOI: https://doi.org/10.1016/j.tsep.2020.100607

EL-BELTAGY, A. – GAMEA, G. R. – ESSA, A. H. A. 2007. Solar drying characteristics of strawberry. In Journal of Food Engineering, vol. 78, no. 2, pp. 456–464. DOI: https://doi.org/10.1016/j.jfoodeng.2005.10.015

ERBAY, Z. – ICIER, F. 2010. A review of thin layer drying of foods: Theory, modeling, and experimental results. In Critical Reviews in Food Science and Nutrition, vol. 50, no. 5, pp. 441–464. DOI: https://doi.org/10.1080/10408390802437063

FORSON, F. K. – NAZHA, M. A. A. – AKUFFO, F. O. – RAJAKARUNA, H. 2007. Design of mixed-mode natural convection solar crop dryers: Application of principles and rules of thumb. In Renewable Energy, vol. 32, no. 14, pp. 2306–2319. DOI: https://doi.org/10.1016/j.renene.2006.12.003

HASAN, M. – LANGRISH, T. A. G. 2016. Development of a sustainable methodology for life-cycle performance evaluation of solar dryers. In Solar Energy, vol. 135, pp. 1–13. DOI: https://doi.org/10.1016/j.solener.2016.05.036

HASSAN, A. – NIKBAKHT, A. M. – FAWZIA, S. – YARLAGADDA, P. K. – KARIM, A. 2023. Assessment of thermal and environmental benchmarking of a solar dryer as a pilot zero-emission drying technology. In Case Studies in Thermal Engineering, vol. 48, article no. 103084. DOI: https://doi.org/10.1016/j.csite.2023.103084

LINGAYAT, A. – CHANDRAMOHAN, V. P. – RAJU, V. R. K. 2017. Design, development and performance of indirect type solar dryer for banana drying. In Energy Procedia, vol. 109, pp. 409–416. DOI: https://doi.org/10.1016/j.egypro.2017.03.041

MEISAMI-ASL, E. – RAFIEE, S. 2009. Mathematical modeling of kinetics of thin-layer drying of apple (var. Golab). In Agricultural Engineering International: The CIGR Ejournal, vol. 11, article no. 1185. Available at: https://cigrjournal.org/index.php/Ejounral/article/view/1185/1228

MELLALOU, A. – RIAD, W. – BACAOUI, A. – OUTZOURHIT, A. 2023. Experimental investigations on drying kinetics and modeling of two-phase olive pomace dried in a hybrid solar greenhouse dryer. In Journal of Thermal Analysis and Calorimetry, vol. 148, no. 12, pp. 5471–5483. DOI: https://doi.org/10.1007/s10973-023-12063-x

MUGI, V. R. – CHANDRAMOHAN, V. P. 2021. Energy, exergy and economic analysis of an indirect type solar dryer using green chilli: A comparative assessment of forced and natural convection. In Thermal Science and Engineering Progress, vol. 24, article no. 100950. DOI: https://doi.org/10.1016/j.tsep.2021.100950

MUSEMBI, M. N. – KIPTOO, K. S. – YUICHI, N. 2016. Design and analysis of solar dryer for mid-latitude region. In Energy Procedia, vol. 100, pp. 98–110. DOI: https://doi.org/10.1016/j.egypro.2016.10.145

ODEWOLE, M. M. – FALUA, K. J. 2021. Modelling of thin-layer drying of osmo-pre-treated red bell pepper. In Acta Technologica

Agriculturae, vol. 24, no. 2, pp. 67–71. DOI: https://doi.org/10.2478/ata-2021-0011

RABHA, D. K. – MUTHUKUMAR, P. – SOMAYAJI, C. 2017. Energy and exergy analyses of the solar drying processes of ghost chilli pepper and ginger. In Renewable Energy, vol. 105, pp. 764–773. DOI: https://doi.org/10.1016/j.renene.2017.01.007

RAJESH, S. – SEKAR, S. – SEKAR, S. D. – MADHANKUMAR, S. 2024. Drying kinetics, energy statistical, economic, and proximate analysis of a greenhouse dryer using different glazing materials for Coccinia grandis drying. In Solar Energy, vol. 284, article no. 113047. DOI: https://doi.org/10.1016/j.solener.2024.113047

ULLAH, I. – HANIF, M. – BASIT, A. – KHATTAK, M. K. – SHAH, S. T. – ULLAH, A. – LODHI, K. – UL-HAQ, I. – ULLAH, I. – AHMAD, M. – ALI, I. – ALI, F. – MOHAMED, H. I. 2022. Performance of two terms exponential model on the drying kinetics of solar-dried tomatoes (*Lycopersicum esculentum* L.) treated with and without chemical preservatives. In Egyptian Journal of Chemistry, vol. 65, no. 3, pp. 455–464. DOI: https://doi.org/10.21608/ejchem.2021.93566.4414